Temperature behaviour of the orange and blue emissions in ZnS:Mn nanoparticles

2002 J. Phys.: Condens. Matter 14 12657

(http://iopscience.iop.org/0953-8984/14/47/336)

INSTITUTE OF PHYSICS PUBLISHING JOURNAL OF PHYSICS: CONDENSED MATTER

J. Phys.: Condens. Matter **14** (2002) 12657–12664 PII: S0953-8984(02)53137-4

Temperature behaviour of the orange and blue emissions in ZnS:Mn nanoparticles

F H Su[1], B S Ma[1], Z L Fang[1], K Ding[1], G H Li[1] and W Chen[2]

[1] National Laboratory for Superlattices and Microstructures, Institute of Semiconductors, Chinese Academy of Sciences, PO Box 912, Beijing 100083, China
[2] Nomadics, Inc., 1024 South Innovation Way, Stillwater, OK 74074, USA

Received 18 October 2002
Published 15 November 2002
Online at stacks.iop.org/JPhysCM/14/12657

Abstract

The temperature dependences of the orange and blue emissions in 10, 4.5, and 3 nm ZnS:Mn nanoparticles were investigated. The orange emission is from the $^4T_1$–$^6A_1$ transition of Mn^{2+} ions and the blue emission is related to the donor–acceptor recombination in the ZnS host. With increasing temperature, the blue emission has a red-shift. On the other hand, the peak energy of the orange emission is only weakly dependent on temperature. The luminescence intensity of the orange emission decreases rapidly from 110 to 300 K for the 10 nm sample but increases obviously for the 3 nm sample, whereas the emission intensity is nearly independent of temperature for the 4.5 nm sample. A thermally activated carrier-transfer model has been proposed to explain the observed abnormal temperature behaviour of the orange emission in ZnS:Mn nanoparticles.

1. Introduction

Semiconductor nanoparticles exhibit peculiar luminescent properties with potential applications, due to quantum confinement [1]. Since Bhargava *et al* [2] first reported that ZnS:Mn nanoparticles show high luminescent efficiency and lifetime shortening, doped nanocrystals of semiconductor have attracted much attention [3–5]. ZnS:Mn nanoparticles have an orange emission at about 2.1 eV (600 nm) and a blue emission band around 2.7 eV (440 nm) under ultra-violet excitation. The orange emission is attributed to the $^4T_1$–$^6A_1$ transition of Mn^{2+} ions and the blue emission is assigned to a donor–acceptor recombination in the ZnS host. Although there is still controversy surrounding the lifetime shortening of the orange emission in ZnS:Mn nanoparticles [6, 7], the luminescence efficiency enhancement in doped nanocrystals of the semiconductor have been confirmed [8, 9]. However, the mechanism for luminescent efficiency enhancement in nanoparticles is still an open question. Bhargava *et al* [2] suggested that the coupling between d-electron states of the Mn^{2+} ion and s–p states of the ZnS host accounts for the lifetime shortening and the luminescence enhancement. However,

some doubts remain because evidence for the hybridization of the d electrons of Mn^{2+} with the s–p states of the ZnS host has not been observed yet.

Temperature dependence of the Mn^{2+} emission in ZnS:Mn nanoparticles has been reported by several groups [10–12]. However, the results are somewhat conflicting. Tanaka and Masumoto [10] have observed that the luminescence intensity of orange emission in ZnS:Mn nanocrystals decreases by approximately 50% from 9 to 300 K. Joly *et al* [11] have also observed a weak decrease in Mn^{2+}-related emission from nanoparticles under 300 nm excitation. However, Yu *et al* [12] have reported that the luminescence intensity of the Mn^{2+} emission from ZnS:Mn nanoparticles increases by about four times with temperature going from 8 to 275 K. However, there has been no report yet on temperature dependence of the blue emission. In this paper, we report a systematic investigation of the temperature behaviour for both the orange and the blue emissions for ZnS:Mn nanoparticles of different sizes.

2. Experiment

Three samples with ZnS:Mn nanoparticles of different sizes were studied. The average sizes of the particles, estimated using a high-resolution transmission electron microscope (HRTEM) and x-ray diffraction (XRD), were approximately 3, 4.5, and 10 nm, respectively. The HRTEM images and the XRD patterns have been published elsewhere [13]. The 3 and 4.5 nm particles were capped with methacrylic acid, while the 10 nm particles were naked, without any capping. Details of the preparation and structure of the samples have been reported previously [13, 14]. Measurements were also made on a commercial bulk ZnS:Mn sample, for comparison.

The photoluminescence (PL) measurements were performed by fixing the samples on the cold finger of a closed-cycle refrigeration system. The temperature can be varied from 10 to 300 K. The 325 nm line of a He–Cd laser was used as the excitation source. The emitted light is dispersed by a JY-HRD1 double-grating monochromator and detected by a cooled GaAs photomultiplier.

3. Results and discussion

Figure 1 shows the PL spectra of three ZnS:Mn nanoparticle samples and a bulk sample recorded at 10 K. The spectra have been normalized according to the intensity of peak M for each sample. The main peak in the PL spectra of the bulk sample is at about 2.11 eV; it is attributed to the $^4T_1$–$^6A_1$ transition of Mn^{2+} ions and is the so-called orange emission [2]. The weak peaks at about 3.3 and 1.6 eV may be due to impurities or defects in bulk ZnS [15] and are not discussed in detail here. The PL spectra of ZnS:Mn nanoparticles consist of two peaks. The peaks at about 2.05 eV are also due to the $^4T_1$–$^6A_1$ transition of Mn^{2+} ions. However, the peak energies for nanoparticles are somewhat lower than those for the bulk sample. This result is consistent with previous reports [2]. The broad band D around 2.7 eV is the so-called blue emission. The blue emission is either attributable to the donor–acceptor pair transition [7] or to the recombination of free carriers at the surface defects [6]. We think that the blue emission is due to the donor–acceptor transition. In our measurements, the intensity of the D band relative to that of peak M increases rapidly with decrease of the particle size. This indicates that the donor state involved in the blue emission is mostly related to the surface states of the nanoparticles, since the surface-to-volume ratio increases when the diameter of the particles decreases. The size dependences of the peak energies for M and D bands are presented in the inset of figure 1. The PL peak energies of bands D increase obviously with decrease of the particle diameter. This change is due to the quantum confinement in the nanoparticles. On the other hand, the energy position of peak M is only weakly dependent on the particle size, as reported previously [13].

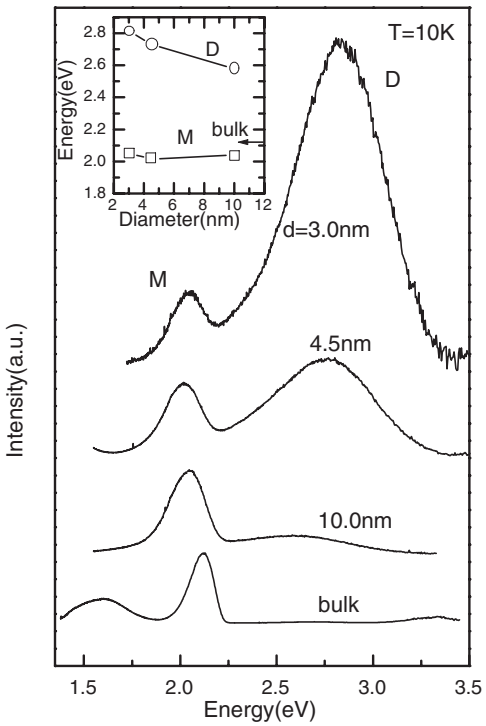

Figure 1. Normalized PL spectra of three ZnS:Mn nanoparticle samples and a bulk sample measured at 10 K. The inset shows the size dependence of the PL peak energies.

The PL spectra for the four samples at different temperatures are shown in figure 2. The spectra were shifted vertically for clarity. The temperature dependences of the peak energies for both M and D bands of the four samples are shown in figure 3. The variation of the ZnS band gap with temperature is also presented for comparison. It can be seen from figures 2 and 3 that the peak position of band M does not change markedly with temperature. On the other hand, the D band has a red-shift with increasing temperature. However, the red-shift of the blue emission does not follow the temperature dependence of the ZnS band gap exactly. Therefore we tentatively assign the blue band to the donor–acceptor transition in ZnS, but the donor state is not a normal shallow state as suggested in [7]. It is more likely that the donor state involved in the blue emission is related to the surface defects of the nanoparticles, as discussed above.

The integrated intensities of Mn^{2+} emissions for all of the samples are shown in figure 4 as functions of temperature. When bands D and M overlap in the spectra, their intensities are determined from a least-squares fit of two Gaussian line profiles. The curves for different samples are shifted vertically for clarity. For the Mn^{2+} emission in the bulk and the 10 nm nanoparticle sample, the PL intensity is exponentially reduced in the higher-temperature region, mainly due to thermally activated nonradiative recombination mechanisms. The temperature dependence of the intensity can be well described on the basis of thermal quenching theory as [18]

$$I(T) = \frac{I(0)}{1 + \frac{e_M}{r_M} \exp(-E_M/k_B T)}, \tag{1}$$

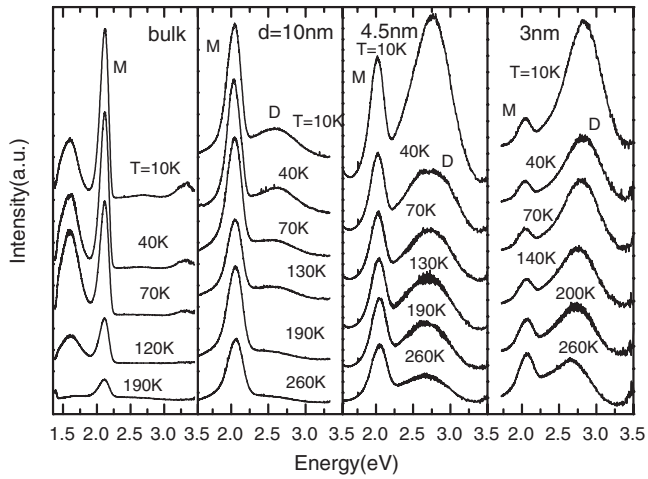

Figure 2. PL spectra for ZnS:Mn nanoparticle and bulk samples at various temperatures.

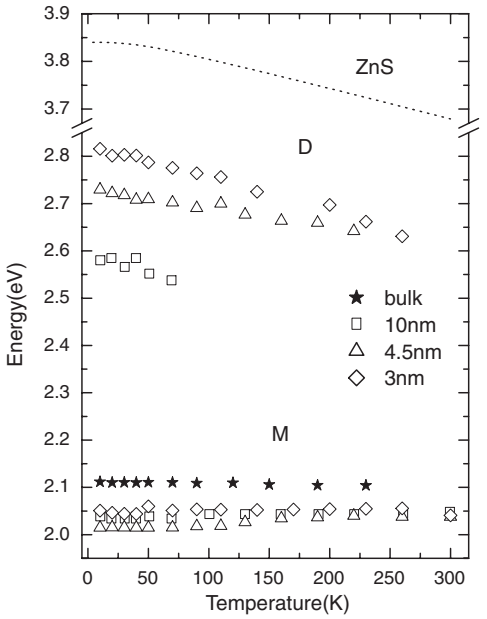

Figure 3. Temperature dependences of the PL peak energies for bands D and M in four samples. The dotted curve shows the temperature dependence for the band gap of bulk ZnS [17].

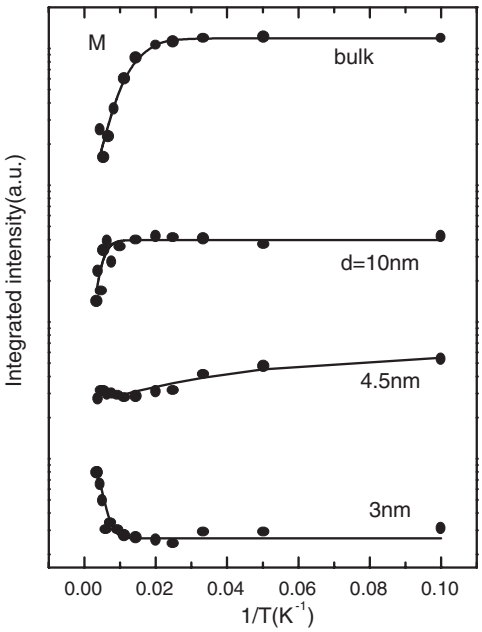

Figure 4. Temperature dependence of the integrated intensity for Mn^{2+} emissions in bulk and nanoparticle samples. The solid curves are the fitting results obtained using equations (1) and (5). See the text for more details.

where E_M is the activation energy for the thermal quenching, k_B is the Boltzmann constant, e_M/r_M is a constant related to the ratio of the nonradiative rate to the radiative rate, and $I(0)$ is the emission intensity at 0 K. A simulation of the intensity for the bulk and the 10 nm sample using equation (1) is presented in figure 4, as solid curves. The parameters used to obtain the simulations are shown in table 1. The E_M obtained for bulk and 10 nm particles are 23 ± 5 and

Table 1. The fitting parameters in the rate equation calculation (see the text for more details).

	Orange emission					Blue emission					
Size	g_M	E_M (meV)	e_M/r_M	E_{M1} (meV)	e_{M1}/r_{M1}	g_D	E_D (meV)	e_D/r_D	E_{D1} (meV)	e_{D1}/r_{D1}	α
3 nm	523					8 303	70 ± 20	21	2 ± 1	1.1	0.9 ± 0.1
4.5 nm	9 322			3 ± 1	1.4	34 571	80 ± 20	70	3 ± 1	3.5	0.7 ± 0.1
10 nm	6 365	60 ± 10	13								
Bulk	11 895	23 ± 5	20								

60 ± 10 meV, respectively. The larger activation energy may be due to the stronger binding of excitons to the Mn^{2+} ions in the nanoparticles than that in bulk.

On the other hand, the temperature dependence of the PL intensities for samples with the 4.5 and 3 nm nanoparticles is different from that for the bulk and the 10 nm sample. The PL intensity of the 4.5 nm sample is only weakly dependent on temperature, while the PL intensity of the 3 nm sample increases rapidly from 110 to 300 K. Weak temperature dependences of Mn^{2+} emissions in ZnS:Mn nanoparticles have been reported by several groups. Tanaka and Masumoto [10] have observed a very weak temperature quenching in the orange luminescence of ZnS:Mn nanocrystals in polymer. They found that the PL intensity of the orange emission from nanoparticles with 3 nm diameter decreases by only about 50% from 9 to 300 K. Joly *et al* [11] have also observed weak temperature dependence of Mn^{2+}-related emission in a 3.5 nm sample under 300 nm excitation. Yu *et al* [12] have reported that the luminescence intensity of the Mn^{2+} emission from 3.6 nm nanoparticles increases by about a factor of four with temperature going from 8 to 275 K. Several mechanisms have been proposed to interpret the abnormal temperature dependence of the Mn^{2+} emission from ZnS:Mn nanoparticles. One of them is energy transfer from the ZnS host to the Mn^{2+} ions. Since both Mn^{2+} and ZnS host-related emissions were observed in our measurements, we can consider the energy-transfer mechanism for nanoparticles in more detail on the basis of the temperature behaviour of bands D and M.

In figure 5 we have plotted the temperature dependences of the integrated intensities of peaks D and M for the 3 nm nanoparticles. The temperature dependence of band D can be divided into two parts. It decreases slowly from 10 to 70 K and then rapidly from 110 to 300 K. The rapid decrease at high temperature can be described by the thermally activated mechanism. The electrons trapped in the donor states are thermally activated to the conduction band. Since the electrons in the conduction band can move more freely in the particles, some of them may be captured by the Mn^{2+} ions and then increase the $^4T_1$–$^6A_1$ transition. The observed increase in intensity of peak M in high-temperature regions confirms the transfer process mentioned above. On the other hand, the slow decrease in intensity of band D may be due to other nonradiative recombination mechanisms with weak temperature dependence. We assume that this process is not included in the carrier transfer from donor states to Mn^{2+} ions. Therefore, the temperature dependence of the orange emission in ZnS:Mn nanoparticles is affected by two factors. One of them is the carrier transfer from donor states and the other is the thermal quenching process as observed in the 10 nm sample. When the first factor is larger (smaller) than the second factor, the intensity of orange emission will increase (decrease) in the higher-temperature region. Further, the intensity of the orange emission will have only weak temperature dependence if the two factors are nearly equivalent.

The above mechanisms can be modelled by a rate equation calculation. We assign N_D and N_M as the numbers of electrons at donor states in the ZnS host and $^4T_1$ levels of Mn^{2+}

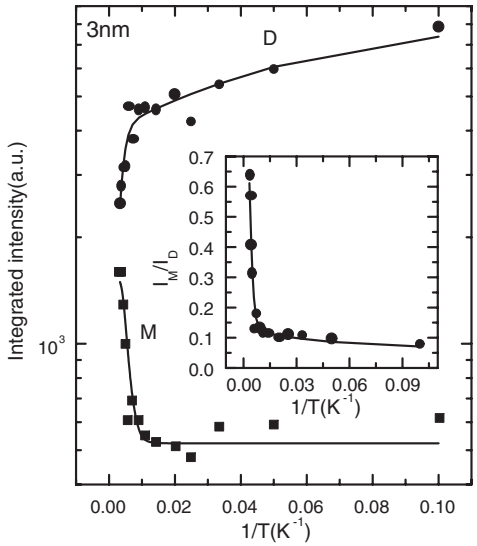

Figure 5. Integrated intensity versus temperature for bands D and M for a sample with 3 nm nanoparticles. The inset shows the intensity ratio of bands M and D as a function of temperature. The solid curves are fitting results obtained using equations (4) and (5).

ions, respectively. Then the rate equations can be expressed as

$$\frac{\mathrm{d}N_D}{\mathrm{d}t} = g_D - N_D r_D - N_D e_D \exp(-E_D/k_B T) - N_D e_{D1} \exp(-E_{D1}/k_B T) \tag{2}$$

$$\frac{\mathrm{d}N_M}{\mathrm{d}t} = g_M - N_M r_M + \alpha N_D e_D \exp(-E_D/k_B T) - N_M e_M \exp(-E_M/k_B T). \tag{3}$$

The first and second terms in the equations describe the generation and radiative recombination processes for electrons in donor states and Mn^{2+} ions, respectively. g_D and g_M are generation rates, r_D and r_M the radiative recombination rates. The third and fourth terms in equation (2) correspond to the rapid and slow decreases of intensity for band D, respectively. The third term in equation (3) represents the transfer process in which the electrons are thermally activated from the donor state and then captured by Mn^{2+} ions. α is the capture factor. The last term in equation (3) describes the thermal quenching of electrons in Mn^{2+} ions. e_D, e_{D1}, and e_M are the emission rates in the corresponding processes. E_D, E_{D1}, and E_M are the activation energies for each process. Under steady conditions the intensity of the blue emission, I_D, can be deduced directly from equation (2) as

$$I_D = N_D r_D = \frac{g_D}{1 + \frac{e_D}{r_D}\exp(-E_D/k_B T) + \frac{e_{D1}}{r_D}\exp(-E_{D1}/k_B T)}. \tag{4}$$

A solid curve in figure 5 represents the least-squares fit of equation (4) to the experimental data for band D. The fitting parameters are listed in table 1. On the other hand, the intensity of the orange emission, I_M, can be presented as

$$I_M = N_M r_M = \frac{g_M + \alpha I_D \frac{e_D}{r_D}\exp(-E_D/k_B T)}{1 + \frac{e_M}{r_M}\exp(-E_M/k_B T)} \tag{5}$$

where I_D is the intensity of band D expressed by equation (4). The experimental data for peak M were fitted using equation (5) and the simulation result for I_D for 3 nm particles. The fitted result is shown by solid curves in figures 4 and 5, respectively. In the fitting, we assume that

the processes of thermal quenching of Mn^{2+} emissions are the same in samples with different particle sizes. Thus the activation energy E_M and the factor e_M/r_M obtained for the 10 nm sample are used in the fitting. Therefore, the adjustable parameters in the fitting are g_M and α, which are also listed in table 1. It is worth noting that the quenching processes may be different in samples with different particle sizes. However, the simulation will be difficult if we include more fitting parameters. This is why we make the approximation mentioned above in the fitting procedure. The inset of figure 5 shows the simulation results for the temperature dependence of the intensity ratios of bands M and D obtained from equations (4) and (5) together with the experimental data. It can be seen from figure 5 that all the simulations are quite good.

A similar fitting procedure was also used for the sample with 4.5 nm particle size. The fitting results for Mn^{2+} emissions are presented in figure 4 as solid curves and the fitting parameters are listed in table 1. Since the intensity of Mn^{2+} emission in the 4.5 nm sample shows a slow decrease from 10 to 50 K, we introduce an additional term similar to the fourth term of equation (2) in the rate equation for N_M in order to obtain best fitting to the experimental results. The parameters for this term are E_{M1} and e_{M1}/r_M, which are also listed in table 1.

Since the blue emission is weak for the 10 nm sample, we assume that the carrier-transfer process can be neglected in the temperature variation of the Mn^{2+} emission. In that case, equation (5) is the same as (1).

The thermal activation energy obtained for electrons in donor states is 70 ± 20 and 80 ± 20 meV for the 3 nm and the 4.5 nm samples, respectively. This indicates that the donor level involved in the blue emissions is located about 70–80 meV under the conduction band edge. The capture factor obtained, α, is 0.9 ± 0.1 and 0.7 ± 0.1 for the 3 nm and the 4.5 nm samples, respectively. It seems that the electrons are more easily captured by Mn^{2+} ions in small particles. This is probably due to the fact that the Mn ions are closer to the surface in smaller nanoparticles. On the basis of the above discussion we can understand the different temperature behaviours of the orange emissions for the four samples. The thermal quenching process is dominant in bulk and the sample with 10 nm nanoparticles. Thus, the intensity of peak M decreases rapidly with increasing temperature. However, the carrier-transfer process dominates the temperature behaviour of Mn^{2+} emission in the 3 nm sample; therefore the intensity of the Mn^{2+} emission exhibits obvious enhancement in the high-temperature region. For the 4.5 nm nanoparticles, the carrier-transfer and thermal quenching processes have nearly same effect on the Mn^{2+} emission. So the intensity of the Mn^{2+} emission is almost independent of temperature.

4. Conclusions

In conclusion, we have investigated the temperature dependence of the PL for ZnS:Mn nanoparticles of different sizes. Two PL peaks were observed for all of the nanoparticle samples. The orange emission is attributed to the $^4T_1$–$^6A_1$ transition of the Mn^{2+} ion and the blue emission is a donor–acceptor pair-related emission of the ZnS host. The intensity of the blue band relative to that of the orange band increases rapidly with decrease in particle size. This indicates that the donor state involved in the blue emission is mostly related to the surface states of the nanoparticles. The PL peak energy of the blue emission increases with decrease in particle size and it shifts to lower energy when temperature increases from 10 to 300 K. However, only weak temperature and size dependences of the PL peak energy for orange emissions were observed. The temperature dependences of the integrated intensities for orange emissions are different for nanoparticles of different sizes. The PL intensity decreases rapidly from 110 to 300 K for the 10 nm sample but increases obviously for the 3 nm sample, whereas the PL intensity is only weakly dependent on temperature for the 4.5 nm sample. A

thermally activated carrier-transfer model has been proposed to explain the observed abnormal temperature behaviour. When temperature increases, the electrons localized on the donor states are thermally activated to the conduction band and some of them are re-captured by Mn^{2+} ions. This effect, along with the process of thermal quenching of electrons on Mn^{2+} ions determines the temperature behaviour of the Mn^{2+} emission in the nanoparticles. The thermal quenching process is dominant in the 10 nm sample, but the carrier-transfer process is dominant in the 3 nm sample. The two effects are almost the same in the 4.5 nm sample, so a weak temperature dependence was observed for this sample.

Acknowledgments

This work was partly supported by the National Natural Science Foundation of China (contract No 60076012) and the Nanometre Science and Technology Programme of the Chinese Academy of Sciences. WC would like to thank Nomadics, Inc., USA, the National Science Foundation (Grant DMI-0132030) and the Air Force Office of Scientific Research (contract No F49620-00-C-0058) for financial support. Bob Hilley is acknowledged for critically reading the manuscript.

References

[1] Wang Y and Herron N 1991 *J. Phys. Chem.* **95** 525 and references cited therein
[2] Bhargava R N, Gallagher D, Hong X and Nurmikko A 1994 *Phys. Rev. Lett.* **72** 416
[3] Yu I, Isobe T and Senna M 1996 *J. Phys. Chem. Solids* **57** 373
[4] Counio G, Esnouf S, Gacoin T and Boilot J-P 1996 *J. Phys. Chem.* **100** 20021
[5] Sooklal K, Cullum B S, Angel S M and Murphy C J 1996 *J. Phys. Chem.* **100** 4551
[6] Bol A A and Meijerink A 1998 *Phys. Rev.* B **58** R15997
[7] Murase N, Jagannathan R, Kanematsu Y, Watanabe M, Kurita A, Hirata K, Yazawa T and Kushida T 1999 *J. Phys. Chem.* B **103** 754
[8] Dinsmore A D, Hsu D S, Gray H F, Qadri S B, Tian Y and Ratna B R 1999 *Appl. Phys. Lett.* **75** 802
[9] Chen W, Sammynaiken R and Huang Y 2000 *J. Appl. Phys.* **88** 5188
[10] Tanaka M and Masumoto Y 2000 *Chem. Phys. Lett.* **324** 249
[11] Joly A G, Chen W, Roark J and Zhang J Z 2001 *J. Nanosci. Nanotechnol.* **1** 295
[12] Yu J, Liu H, Wang Y, Fernandez F E and Jia W 1998 *J. Lumin.* **76&77** 252
[13] Chen W, Sammynaiken R, Huang Y, Malm J-O, Wallenberg R, Bovin J-O, Zwiller V and Kotov N A 2001 *J. Appl. Phys.* **89** 1120
[14] Chen W, Li G H, Malm J-O, Huang Y, Wallenberg R, Han H, Wang Z P and Bovin J O 2000 *J. Lumin.* **91** 139
[15] Thong D D and Goede O 1983 *Phys. Status Solidi* b **120** K145
[16] Murase N, Jagannathan R, Kanematsu Y, Watanabe M, Kurita A, Hirata K, Yazawa T and Kushida T 1999 *J. Phys. Chem.* B **103** 754
[17] Tsay Y F, Mitra S S and Vetelino J F 1973 *J. Phys. Chem. Solids* **34** 2167
[18] Kosai K, Fitzpatrick B T, Grimmeiss H G, Bhargava R N and Neumak G F 1979 *Appl. Phys. Lett.* **35** 194